Available online at www.sciencedirect.com
SCIENCE DIRECT®
ELSEVIER
Nuclear Instruments and Methods in Physics Research B 211 (2003) 122–132
NIM B
Beam Interactions with Materials & Atoms
www.elsevier.com/locate/nimb

Study of the effect of high electronic excitations in quasicrystals irradiated with heavy ions ☆

Gerrit Coddens [a,*], Annie Dunlop [a], Hichem Dammak [b], Ratnamala Chatterjee [c], Yvonne Calvayrac [d], Marianne Quiquandon [e], Erik Elkaïm [f], Mark Gailhanou [f], Stéphan Rouzière [f]

[a] *Laboratoire des Solides Irradiés, CEA/CNRS/Ecole Polytechnique, F-91128 Palaiseau Cedex, France*
[b] *Laboratoire S.P.M.S., Ecole Centrale de Paris, Grande Voie des Vignes, 92295 Châtenay-Malabry Cedex, France*
[c] *Department of Physics, Indian Institute of Technology, New Delhi 110 015, India*
[d] *CECM/CNRS, F-94407 Vitry Cedex, France*
[e] *LEM-CNRS/ONERA, BP 72, F-92322 Châtillon Cedex, France*
[f] *LURE, F-91405 Orsay Cedex, France*

Received 14 November 2002; received in revised form 13 March 2003

Abstract

We have studied the effect of irradiation with 900 MeV Pb and 780 MeV Xe ions on quasicrystals $Al_{62}Cu_{25.5}Fe_{12.5}$ and the related cubic α-phase $Al_{55}Cu_{27}Fe_{11}Si_7$. The fluences ranged from 10^{10} to 5.8×10^{13} ions/cm^2. Irradiations were performed at 80 K and at room temperature. The structural changes induced by the electronic excitations were studied by high-resolution X-ray diffraction. Whereas one might have expected the irradiations to induce important structural transformations, e.g. a phase transition from an icosahedral to a rhombohedral phase, only minor structural modifications are observed in the icosahedral phase and none in the α-phase. The defects created are not phasonic. Our results suggest a remarkable structural stability of these phases with respect to heavy-ion irradiation.

PACS: 61.72.Dd; 61.80.Jh; 61.82.Bg; 61.44.Br
Keywords: Swift-heavy-ion irradiation; Electronic excitation; Quasicrystals; Approximants; X-ray diffraction; Phason strain

1. Introduction

The present work is a continuation of efforts [1] to study the effect of heavy-ion irradiation on quasicrystals (QCs). In this paper we present our data on well annealed icosahedral $Al_{62}Cu_{25.5}Fe_{12.5}$ and a related crystalline phase, the cubic α-phase $Al_{55}Cu_{27}Fe_{11}Si_7$. More precisely we are searching for structural modifications induced in these samples by high-energy projectiles in the electronic energy deposition regime. The two types of samples (of 22 ± 2 μm thickness) were irradiated with 900 MeV Pb and 780 MeV Xe ions delivered by the GANIL facility at Caen, France. In $Al_{62}Cu_{25.5}Fe_{12.5}$

☆ The irradiations were performed in Caen (France) using the GANIL facility.

* Corresponding author. Tel.: +33-1-69-33-45-09; fax: +33-1-69-33-30-22.
E-mail address: gerrit.coddens@polytechnique.fr (G. Coddens).

0168-583X/$ - see front matter © 2003 Elsevier B.V. All rights reserved.
doi:10.1016/S0168-583X(03)01210-2

these ions have projected ranges of 31 and 36 μm respectively, so that they are not stopped in the targets. Within the sample thickness the average linear rates of energy deposition in elastic collisions $(dE/dx)_n$ and in electronic processes $(dE/dx)_e$ are respectively 0.1 and 40 keV/nm for Pb ions and 0.04 and 25 keV/nm for Xe ions, such that nuclear elastic collisions can almost be neglected. Irradiations were carried out at 80 K and at room temperature using an ion flux smaller than 10^8 ions/cm^2 in order to avoid significant temperature increases under the ion beam. The structural changes in the samples after irradiations up to fluences of 10^{10} to 5.8×10^{13} ions/cm^2 were studied at room temperature by high resolution X-ray diffraction.

Our results are complementary to those obtained by Wang et al. [2] who irradiated icosahedral QCs of the same composition $Al_{62}Cu_{25.5}Fe_{12.5}$ with 120 keV Ar^+ ions and with 1 MeV electrons. The heavy-ion energies correspond to exactly the opposite regime as was explored in our experiments, i.e. they are dominated by the *nuclear* stopping power rather than by the electronic one. In a first series of experiments Wang et al. irradiated the samples at room temperature with Ar ions. The fluences ranged between 10^{11} and 5×10^{16} ions/cm^2. The structural modifications induced by the irradiations were characterized by electron microscopy. The authors observed a transition towards a microtwinned B2-based CsCl-type structure. The B2-type microtwins showed icosahedral orientational relationships. They also studied how these irradiated samples could be annealed to a less perfect icosahedral phase by a successive temperature treatment (for temperatures up to 1000 K). In the other experiments the samples were irradiated at higher temperatures, up to 810 K with fluences up 2×10^{15} Ar ions/cm^2, or up to 890 K with up to 3.2×10^{23}/cm^2 1 MeV electrons.

2. Phase diagram of AlCuFe

There are several reasons why the ternary alloy AlCuFe was selected for this study on QCs. It is one of the alloys in which samples are routinely obtained with high structural perfection and in large quantities. It was historically the first icosahedral phase that exhibited resolution-limited sharp Bragg peaks. The QC $Al_{62}Cu_{25.5}Fe_{12.5}$ is for all these reasons one of the best studied. It functions as a standard. In order to make the various studies comparable, everybody has worked on the same phases (especially AlCuFe and AlPdMn). Hence, a large amount of studies on the various physical properties of $Al_{62}Cu_{25.5}Fe_{12.5}$ have been carried out. Especially, the structural refinement of this phase is in the most advanced stage of all icosahedral QCs.

A second reason to select $Al_{62}Cu_{25.5}Fe_{12.5}$ can be appreciated by inspecting its phase diagram at 700 °C, as shown in Fig. 1 [3]. We see that in a very small range of concentrations there is a plethora of phases. This phase diagram has been studied in great detail and is well-known. E.g. it is well established that the rhombohedral phase of

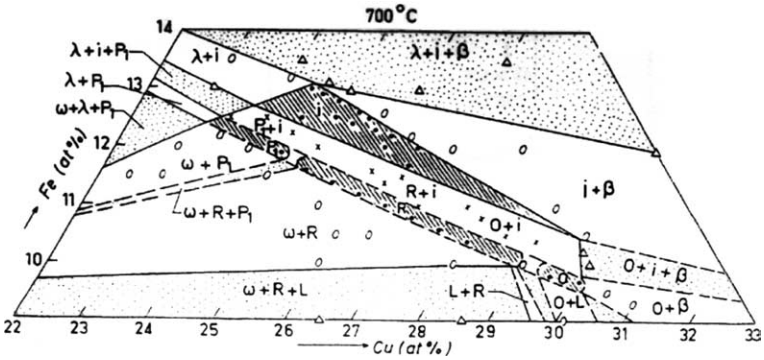

Fig. 1. Phase diagram of AlCuFe at 700 °C as taken from [3]. Here i notes the icosahedral phase, R the rhombohedral phase, P_1 a first pentagonal phase, P_2 a second pentagonal phase, β a cubic beta-phase, O an orthorhombic phase.

composition $Al_{62.5}Cu_{26.5}Fe_{11.5}$ transforms to an icosahedral phase above 710 °C. The transition seems to be partly reversible but there is a strong hysteresis. The systems in this tiny concentration area are thus highly sensitive to experimental parameters and may undergo phase transitions between each other. The structure acts like a magnifying glass for minute changes in the energy balance of the structure.

When this study was started it was considered to be possible that heavy-ion irradiation in the high electronic excitation regime, which can induce atom mobility in quite a number of metallic targets [4], might result in such phase transitions in QCs. There are several indications that the phase transitions in AlCuFe could be governed by (phason) atomic jumps. Such jumps have been observed experimentally at the temperatures where the phase transitions happen [5]. They are then very fast but require the assistance from an unknown mechanism which has an activation energy of the order of 0.2–0.6 eV. Displacing an atom by a phason jump corresponds to the creation of a structural defect that is typical of QCs and has not a counterpart in regular solids: the atom neither jumps to an interstitial position nor to a previously existing vacancy site. The sites the atoms jump to are readily available in large concentrations as an intrinsic part of the structure of QCs, and do not have to be created. Only some assistance energy has to be delivered to the system in order to prepare the jump. The defect is thus expected to cost very little energy, and one anticipates that it should not be too difficult to displace atoms in QC, a fact that is confirmed by the high jump rates observed in phason dynamics. On the other hand the jumps appear to be totally blocked in the cubic α-phase $Al_{55}Cu_{27}Fe_{11}Si_7$ which is obtained from the icosahedral phase $Al_{62}Cu_{25.5}Fe_{12.5}$ by substituting a small part of the Al by Si, and by slightly modifying the balance between Cu and Fe concentrations.

3. Experimental

The samples were thin flakes of the canonical icosahedral phase i-$Al_{62}Cu_{25.5}Fe_{12.5}$ and of the cubic alpha phase α-$Al_{55}Cu_{27}Fe_{11}Si_7$. These flakes were pieces of ribbons obtained by meltspinning, as described in [3]. Their thicknesses are 22 ± 2 μm. They were annealed at 800 °C for 2 h (for the i-phase), and at 650 °C for 20 h (for the α-phase). The resulting phases are well known and have been described in detail by Quiquandon et al. [3]. More specifically, it has been verified that diffractograms of samples from the same batch are identical to the very best attainable resolution. The samples were mounted in a liquid-nitrogen cryostat. Within this cryostat, at the position in the heavy-ion beam, an assembly of copper plates is fixed in good thermal contact onto the cold finger. The samples were fixed on these copper plates. Along the trajectory of the heavy ion in the sample there is a cylindrical volume wherein the energy is deposited in the form of ionizations and electronic excitations. At the maximal fluence of 5.8×10^{13} heavy ions/cm^2 these cylindrical volumes overlap, such that the whole of the sample has then been subjected to electronic excitation.

After slowly taking the samples back to room temperature, the effect of the irradiations on their structure was studied by high-resolution X-ray diffraction. The best results were obtained with an incident X-ray beam of 12.398 keV ($\lambda = 1$ Å) on a four-circle diffractometer installed at the beam line DW22 of the Laboratoire pour l'Utilisation du Rayonnement Electromagnétique (LURE), Orsay, France. But also several characterizations (before and after the irradiations) were made at the beam line H10 of LURE (with 6.92 keV X-rays ($\lambda =$ 1.7917 Å)) and at the rotating anode source of the Ecole Centrale de Paris, Châtenay-Malabry, France (with K_αCu X-rays ($\lambda = 1.54056$ Å)). Some of these charaterizations were carried out within days after the irradiation, while the final measurements on DW22 were made 13 months after the irradiation. We did not come across any evidence that would suggest that the structure of the samples has evolved over that period [6].

During the first X-ray tests it appeared that the polycrystalline flakes were highly textured: The surface of the flakes imposes strong preferential orientations on the grains. We prefered to perform the X-ray characterizations on such textured samples rather than reducing them to a fine powder by means of a mortar for two reasons: (1)

the mechanical treatment might have an effect on the structure of the sample, as was e.g. reported by Boudard et al. [7]; (2) it is not easy to collect the powder from a small flake as most of it sticks to the mortar. Hence, in order to average over a significant number of grains, the sample has to be rotated (at a few Hz) during the data acquisition.

The vertical beam divergence at DW22 was better than 0.1 mrad. In a standard powder diffractometer set-up, X-rays scattered by different parts of the sample reach the detector with slightly different scattering angles. This effect was aggravated by the difficulties we experienced to reproducibly put the sample always at the same height in the beam. In fact, the latter involved too much personal judgement. The flakes are not really flat and rather present a bent profile, their thickness is not homogenous, their surfaces are not rigorously parallel with the surface of the glass plate backing, and the thickness of the glue between the glass plate and the sample is also not homogeneous. After several trials of aligning them as well as possible with the aid of a small optical telescope it turned out that we could not render our X-ray measurements sufficiently reproducible. Therefore on beamline DW22 a high-resolution set-up was used with a Ge111 crystal analyser collecting the diffracted beam. This set-up is well suited for our measurements on irregularly shaped samples since the Bragg peaks positions and shapes obtained are then almost insensitive to the height of the samples [8]. It resulted in a substantial improvement of the resolution and perfect reproducibility. Of course there was a concomittant loss of intensity, which we counterbalanced by increasing the measuring times. Typical measuring times were of the order of 30 min for a single run on an icosahedral sample. Such a run contained roughly 180 data points and consisted of three θ–2θ scans (for the three Bragg peaks) with angular steps of $\Delta 2\theta = 0.004°$.

For the characterization we focused our attention on the three Bragg peaks of the icosahedral phase with indices (N/M) 6/9, 7/11 and 8/12 in the Cahn–Shechtman–Gratias indexing scheme, [9] and two Bragg peaks of the α-phase that occur in the same Q-region. This region in Q-space was selected for its high sensitivity with respect to structural changes. In fact, the three icosahedral Bragg peaks mentioned have rather large $Q_\perp$-values (see Table 1). E.g. the transition to the rhombohedral approximant phase discussed in Section 2 leads to a very clear splitting of the 7/11 Bragg peak (see e.g. [5] in [3]) as can also be appreciated from Table 1, where we included information about the rhombohedral phase for comparison [10].

Often scans have been repeated with identical measuring conditions in order to check reproducibility. However, these spectra sometimes revealed different signal/background ratios due to long-period drift in the beam alignment. To minimize such effects, the beam was regularly realigned, but over night such drifts did occur. In the subsequent data analysis, we did not combine data with different S/N ratios to yield single data sets, but treated the files separately.

4. Data analysis

In a first approach we tried to fit the data by a Voight profile with a linear background contribution, using the program FULLPROF developed by J. Rodriguez-Carvajal [11]. The underlying idea was that we tried to check if a spectrum could consist of a Gaussian-shaped Bragg peak and some Huang scattering, which in a first approach

Table 1
Characteristics of the Bragg peaks studied in the icosahedral phase

N	M	$Q_\parallel$ (Å^{-1}) (icosahedral phase)	$Q_\perp$ (Å^{-1}) (icosahedral phase)	$Q_\parallel$ (Å^{-1}) (rhombohedral phase)
6	9	0.266823	0.0629897	0.26524, 0.26646, 0.26851
7	11	0.293027	0.0427521	0.29116, 0.29591
8	12	0.308107	0.0727342	0.30207, 0.30946, 0.31114, 0.31119

The corresponding data for the rhombohedral phase $Al_{62.5}Cu_{26.5}Fe_{11.5}$ are given for comparison.

might be described by a Lorentzian profile. [1] The width and relative intensity of the intervening Lorentzian would then parametrize the amount of disorder created in the sample. While it was possible to obtain satisfactory fits by this Voigt approach, the fit parameters obtained vary erratically with the measuring conditions. One can rationalize this by stating that the widths of the Gaussian and the Lorentzian contributions are very similar, which makes the mathematical problem ill-conditioned as e.g. described by Sivia et al. [13]: Intensity can be transferred from one contribution to the other without appreciably changing the lineshape of the total signal. The statistical fluctuations in the data can result then in meaningless variations in the intensities of the two components.

In conformity with this reading, the spectra could be fitted with a single Lorentzian and a linear background only. To facilitate the comparisons, we normalized all spectra to unit maximum intensity before performing the fits. This does not imply a lack of information, as the precise amount of diffracting matter in the beam is not known. As the peak positions are virtually constant, this means that in practice the fits depend on a single physical parameter, which is the width of the Lorentzian. The results are reasonably satisfactory except for one case (the second peak in the spectrum obtained by irradiating the sample at 80 K up to a fluence of 5.8×10^{13} Pb ions). In some cases the fits were perfect, while in most cases there were some minor imperfections due to a slight asymmetry in the peak shape. Fig. 2 gives representative illustrations of the quality of a bad and a good fit.

To acknowledge for the asymmetry we fitted the data still in a third way with a "distorted Lorentzian" of varying width:

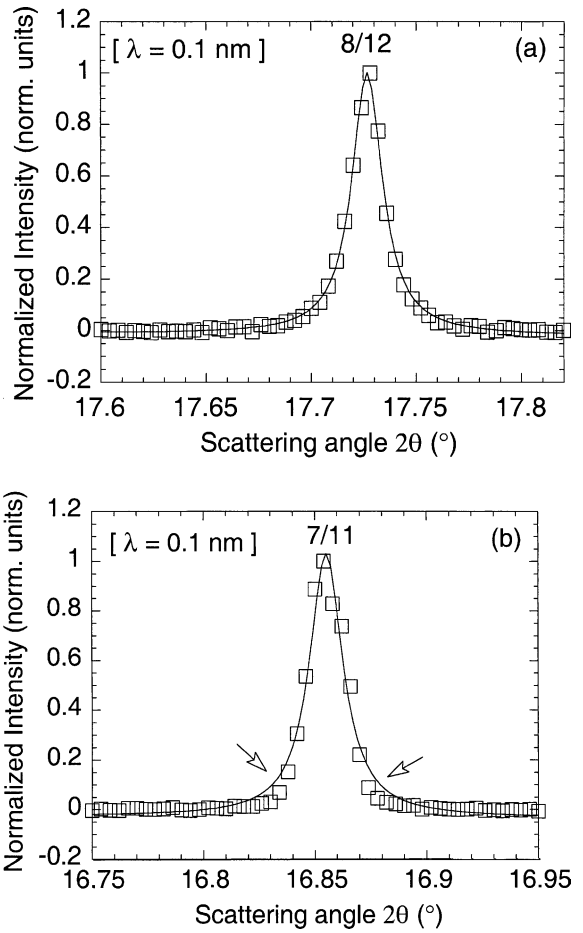

Fig. 2. Typical good (a) and bad (b) Lorentzian fits. The data are from icosahedral samples irradiated with (a) 10^{12} Pb ions/cm^2 at 80 K (8/12 Bragg peak) and with (b) 5.8×10^{13} Pb ions/cm^2 at 80 K (7/11 Bragg peak). The open arrows highlight the inadequacy of the fit.

[1] Ideally, the correct profile for a fit of Huang scattering in QCs should be given by inverting analytically the matrix $\mathbf{C}(\mathbf{k})$ in the formalism developed by Jarić and Nelson [12]. Here $\mathbf{k} = \mathbf{Q} - \mathbf{G}$ is the relative position of the scattering vector with respect to the nearby Bragg peak $\mathbf{G}$. These expressions must then further be averaged over all directions of $\mathbf{Q}$, and expressed in terms of $Q - G \neq |\mathbf{Q} - \mathbf{G}|$. Making such a powder average tacitly assumes that the sample does not exhibit any texture, while this is actually very conspicuously not true for our QC ribbons: As we already mentioned, they exhibit preferential orientations with respect to the surface. Furthermore, even if one limits the analytical inversion of $\mathbf{C}(\mathbf{k})$ to the case that only the phason–phason or phonon–phonon elastic constants are considered, this first step of the calculation already proves to be a very cumbersome task in its own right. We thus took a shortcut to this theoretical exercise and assumed that the Voigt profile would be a good first-order approximation. (Of course, this first-order approach can never reproduce the small amount of asymmetry we observed. Asymmetries in the diffuse scattering are traditionally studied by representing the data on a logarithmic-linear scale, but our scans did not contain enough data points in the wings of the peaks to afford such a study. In the approach with a Voigt profile and a linear background the asymmetry is admittedly mistreated as physically meaningless by relegating it to the background.)

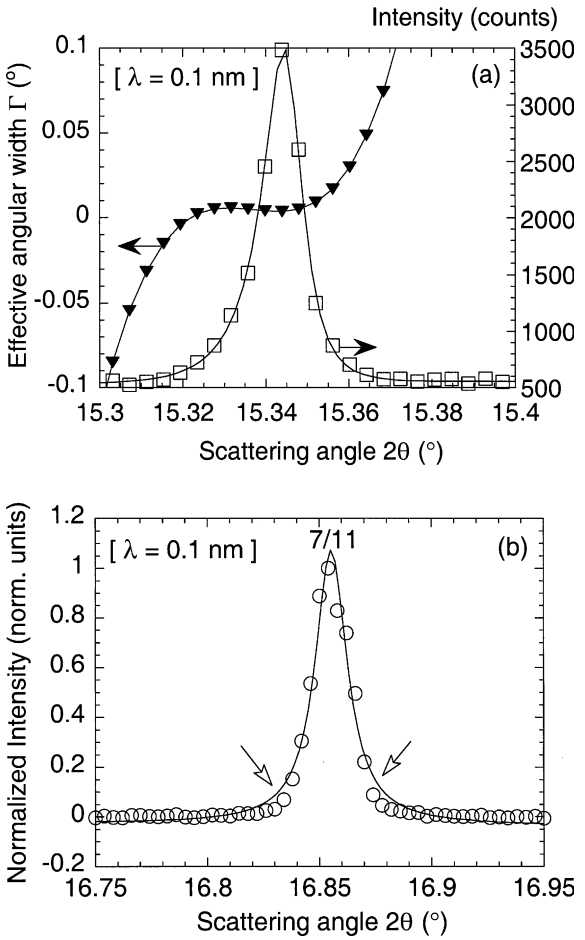

Fig. 3. Typical good (a) and bad (b) distorted-Lorentzian fits. In case (a) the data are from an icosahedral sample irradiated with 10^{11} Pb ions/cm^2 at 80 K (6/9 Bragg peak). The open squares represent the measured data, the filled triangles represent the effective half width Γ used in Eq. (2). In case (b) the data are from an icosahedral sample irradiated with 5.8×10^{13} Pb ions/cm^2 at 80 K (7/11 Bragg peak) and the improvement with respect to a plain Lorentzian fit is poor (see Fig. 2(b)). Here again the open arrows highlight the inadequacy of the fit.

$$S(Q) = c_1 + c_2(Q - Q_0) + \mathscr{I}/((Q - Q_0)^2 + [\gamma_0 + \gamma_1(Q - Q_0) + \gamma_2(Q - Q_0)^3]^2). \quad (1)$$

i.e. we replaced the traditional constant width Γ (HWHM) by a polynomial expression $\gamma_0 + \gamma_1(Q - Q_0) + \gamma_2(Q - Q_0)^3$. The fit parameters are the backgound parameters c_1, c_2, the peak position and intensity Q_0, $\mathscr{I}$, and the three width parameters γ_0, γ_1, γ_2. This is of course a purely mathematical description, a priori without any physical justification. Typical good and bad results are shown in Fig. 3. In these fits a negative width is equivalent with a positive width of the same amplitude. We can see from this representation that the width remains constant over the central part of the peak, and increases in the tails. This is in reality a small refinement with respect to the approach based on a simple Lorentzian as the intensity in the tails is rather low. In order to facilitate the interpretation of the results, we diminished in a second stage the number of parameters in these fits: we first determined the peak shape in the non-irradiated samples according to Eq. (2) and took its parameters as fixed values ($\gamma_0^0, \gamma_1^0, \gamma_2^0$) in a description of the other data by

$$c_1 + c_2(Q - Q_0) + \mathscr{I}/((Q - Q_0)^2 + [\gamma_0^0 + \gamma_1^0 W(Q - Q_0) + (\gamma_2^0 W(Q - Q_0))^3]^2), \quad (2)$$

which again only depends on one width (broadening) parameter W. The other fit parameters are c_1, c_2, Q_0. The parameter W gives a monotonic, but non-linear description of the width variations. The quality of the corresponding fits is excellent. They confirm the main tendencies observed with the purely Lorentzian fits. Therefore, we will present our results only in terms of the values 2Γ obtained with a plain Lorentzian fits ($S(Q) \propto (1/\pi)\Gamma/((Q - Q_0)^2 + \Gamma^2)$), rather than the values from fits based on Eq. (1) or (2).

5. Results for the icosahedral phase

Table 2 summarizes our results for the icosahedral phase. Sometimes two entries for the same experimental conditions are given. They represent then the strongest deviations found within a series of repeated measurements on the same sample in order to check reproducibility. A first immediately obvious result is that the peak positions of the three Bragg peaks hardly change. The shifts extracted from the fits we described above were less than or of the order of the scan step of 0.004°. For the 6/9 peak the values ranged between 15.335° and 15.342°, for the 7/11 peak between 16.853°

Table 2
Positions 2θ (°) and widths (FWHM) 2Γ (0.001°) of the Bragg peaks in the icosahedral phase

Ion	$(dE/dx)_e$ (keV/nm)	Fluence (ions/cm^2)	Irradiation temperature (K)	Peak 6/9		Peak 7/11		Peak 8/12	
				2θ	2Γ	2θ	2Γ	2θ	2Γ
–		0		15.342	13.4	16.860	8.4	17.729	12.4
Pb	40.0	10^{11}	80	15.337	9.0	16.855	10.4	17.728	11.4
Pb	40.0	10^{12}	80	15.334	17.6	16.857	16.4	17.727	17.8
Pb	40.0	5.8×10^{13}	80	15.339	14.4	16.853	13.6	17.724	12.8
				15.339	13.4	16.857	17.8	17.725	15.4
Xe	25.0	10^{11}	80	15.341	14.4	16.857	13.4	17.726	11.8
				15.335	12.8	16.856	12.8	17.726	12.4
Xe	25.0	10^{12}	80	15.340	12.6	16.857	10.8	17.727	10.8
Xe	25.0	10^{13}	80	15.342	18.6	16.857	17.0	17.725	20.0
Xe	25.0	10^{13}	300	15.341	13.6	16.857	13.8	17.728	15.4

and 16.860°, and for the 8/12 peak between 17.724 and 17.729°.

That the Lorentzian fits worked so well is a very important result. It means that the principal effect of irradiation is a global broadening of the line shape, rather than transfering intensity from the centre of the Bragg peak to its wings. This is further confirmed by the quality of the fits obtained with the procedure described in Eq. (2), which is also based on the idea of a global broadening. In Fig. 4 these two main observations are illustrated

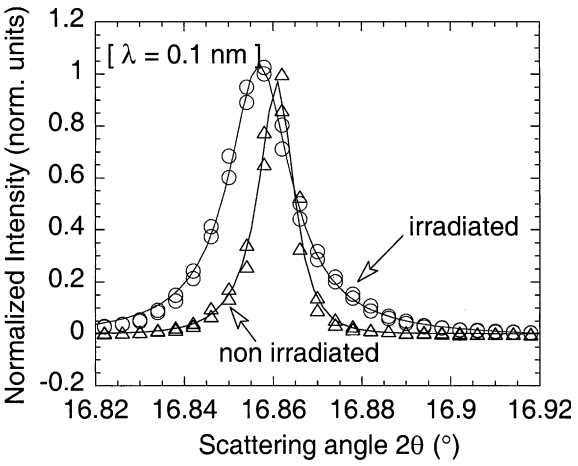

Fig. 4. Comparison of the data from the icosahedral sample irradiated with 10^{13} Xe/cm^2 at 80 K (open circles) and from a non-irradiated icosahedral sample (open triangles), to show that the effects of irradiation are clearly visible even with the unaided eye (7/11 Bragg peaks). The peak is roughly twice as broad in the irradiated sample. There is a clear but very small shift of the peak position towards lower scattering angles (reflecting a small lattice expansion).

in a comparison of a non-irradiated sample and the sample that showed the strongest effects (10^{13} Xe ions/cm^2 at 80 K). The shift of the peak position is of the order of one angular increment during the scans. These observations render it improbable that the disorder could be interpreted in terms of Huang scattering.

It is perhaps instrumental to emphasize that this global broadening is minute (see above): it can only be resolved with a resolution that is available on a synchrotron radiation facility, not with other sources of X-rays. The largest broadening we observed is about twice the peak width we find in a non-irradiated sample. There is no trace in the spectra of any formation of other phases, such as the rhombohedral approximant which has its Bagg peaks at Q-values which at this scale of resolution look far away. For comparison, we show in Fig. 5(a) the diffraction diagram obtained for the non-irradiated rhombohedral phase under identical experimental conditions. It may be noted here for completeness that the preliminary runs with a more coarse resolution also failed to detect any sign of the presence of other phases, such that we can be sure that we did not miss evidence for the presence of such phases because the resolution would have been too good (Fig. 5(b)) or our scan intervals too narrow.

Another important result can be observed in Table 2. While the three Bragg peaks have different $Q_\perp$ values their global broadenings for a given measuring condition are practically identical, which suggests that they do not depend on the phason elastic constants.

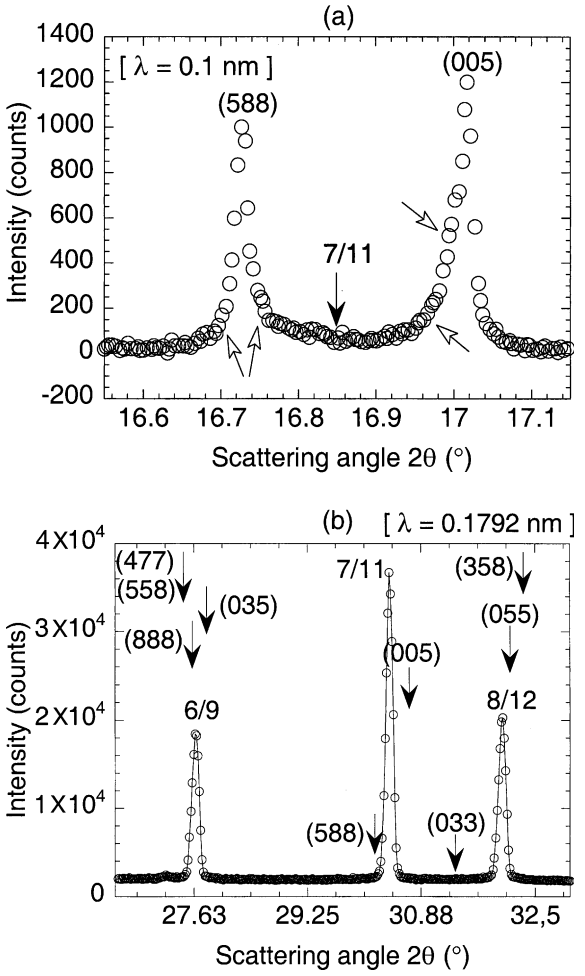

Fig. 5. (a) Spectrum of a non-irradiated rhombohedral phase (sample $Al_{62.8}Cu_{26}Fe_{11.2}$ annealed for 3 days at 705 °C). The peaks have indices (5 8 8) (left) and (0 0 5) (right), respectively. The position of the 7/11 icosahedral Bragg peak is shown by the full arrow. The rhombohedral peak positions are thus clearly shifted with respect to those of the icosahedral phase. The shapes of the rhombohedral peaks (open arrows) render it impossible to study effects of the same order of magnitude as one observes in the icosahedral phase upon irradiation. That no traces of this or any other phase are present in the irradiated icosahedral phase is illustrated in (b) which shows the spectrum of an icosahedral phase after irradiation with 10^{13} Xe/cm^2 at 80 K as measured at H10 with a lower resolution. The arrows show the positions and indexing for the Bragg peaks of the rhombohedral phase.

These broadenings seem to decrease slightly at low fluences before they start to increase at higher fluences. The threshold for this increase lies slightly lower for Pb ions (10^{11} ions/cm^2) than for Xe ions (10^{12} ions/cm^2). (i) The dependence of the peak broadenings on the irradiation conditions is reminescent of what one can observe in some amorphous metals [14], i.e. (1) after irradiation at moderate fluences with GeV ions, a local atomic rearrangement of the structure is observed in the amorphous alloy, (2) after irradiation at high fluences, radiation damage accumulates and disorder is introduced. (ii) The broadenings of the peaks are stronger after irradiation at low temperature than at room temperature. This can be explained by the fact that the defects created can be mobile at 300 K and partially recombine, while at 80 K their mobilities are strongly reduced. (iii) Finally, the effects produced are stronger after irradiations with Pb than after Xe irradiation, which is directly related to the fact that the electronic stopping power of Pb ions is larger than that of the Xe ions.

6. Results for the cubic α-phase

The peaks that we studied have the Miller indices (3 2 0) and (3 2 1). As such they correspond to the 7/11 and 8/12 Bragg peaks of the icosahedral phase. In fact [15] in the cubic α-phase the icosahedral Bragg peak 6/9 splits into the doublet (3 1 0) and (2 2 2), while 8/12 splits into (3 2 1) and (4 0 0). The Bragg peak 7/11 remains a singlet and corresponds to the peak (3 2 0). The cubic phase is even less affected by the heavy-ion irradiation (Table 3) than the QCs. Not only the peak positions but also the widths do not show any appreciable variation. The fits were subject to the same problems as for the icosahedral phase. Lorentzian fits worked well except sometimes in the tails. The fits with Eq. (2) worked perfectly (Fig. 6).

7. Discussion

It can be said that the effects of disorder we observe are really small. For comparison we show in Fig. 7 the broadening of the peaks one can observe in an as-cast QC sample after quenching from the melt. These data were taken in a

Table 3
Positions 2θ (°) and widths (FWHM) 2Γ (0.001°) of the Bragg peaks in the cubic alpha phase

Ion	$(dE/dx)_e$ (keV/nm)	Fluence (ions/cm^2)	Irradiation temperature (K)	Peak (3 2 0)		Peak (3 2 1)	
				2θ	2Γ	2θ	2Γ
–		0		16.829	11.2	17.471	12.2
Xe	25.0	10^{12}	80	16.829	12.6	17.471	13.4
Xe	25.0	10^{13}	80	16.829	13.2		
						17.471	13.2
Xe	25.0	10^{13}	300	16.829	12.2		
				16.829	12.6	17.471	12.8

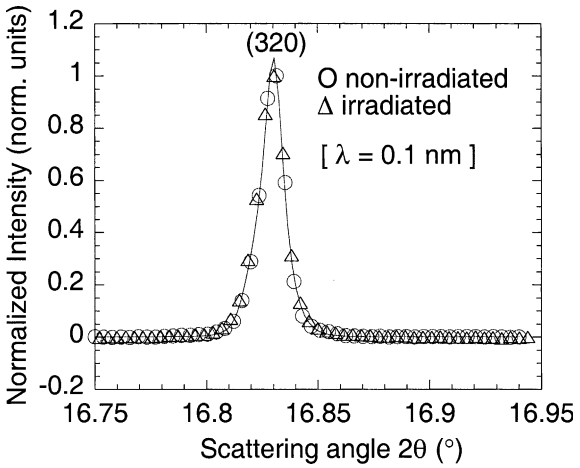

Fig. 6. Comparison of the spectra of a cubic α-phase irradiated with 10^{12} Xe ions/cm^2 at 80 K (open triangles) and a non-irradiated cubic α-phase (open circles). A fit with a distorted Lorentzian profile (Eq. (2)) to the data from the non-irradiated sample is shown to guide the eye.

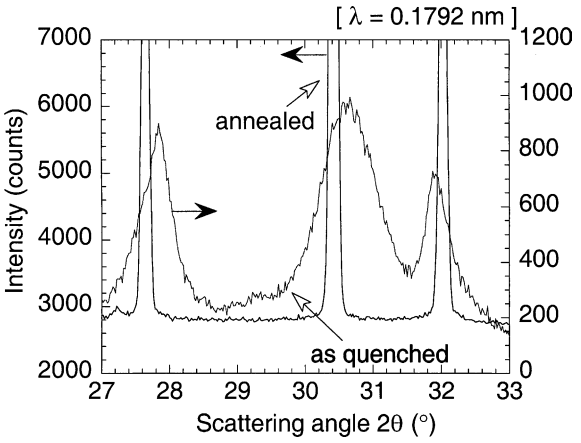

Fig. 7. Comparison of the spectra of an imperfect icosahedral sample obtained by quenching from the melt without any annealing and of an annealed perfect icosahedral sample of the same composition (as measured on H10). The widths in the quenched sample are much larger than those we were able to produce by irradiation.

diffractometer set-up with a poorer resolution, but the resolution remains much better than the widths of these peaks. These peaks are thus orders of magnitude broader than in our observations. We may note that it is interesting to confront the orders of magnitude we obtained with what one knows about the way the electronic energy deposited by heavy ions into the sample is relaxed. Authors now agree that Coulomb explosion and thermal spikes are early and late aspects of the same decay process [16] and that during the relaxation of the energy deposited in the electronic processes a radial shock wave is generated along the trajectory of the heavy ion [17]. In our experiment we can get a crude estimate of the pressures developed in these shock waves as follows. [2] Our experimental results are reminiscent of the behaviour of QC under pressure as reported by Lefebvre et al., Sadoc et al. and Joulaud et al. [18]: The icosahedral phase is remarkably stable under

[2] We may note that this is only a crude argument. There are important differences with a measurement under static hydrodynamical pressure. During the shockwave the applied pressure is not static. It is not homogeneous throughout the sample. It is not hydrodynamical, but rather radial with respect to the path of the ion. And finally, the grains have special orientations with respect to the applied pressure, due to the texture in the sample.

pressure. The main effects of applied pressure are a reduction of the lattice parameter (under very high pressures) and a global broadening of the peaks. Especially, after release of the high pressure, the initial peak positions are recovered and only a global broadening of the peaks is observed. The width of the 8/12 peak e.g. shows a linear behaviour between 0 and 35 GPa. At 35 GPa the width is twice its value at ambient pressure. The two other peaks exhibit only a slow variation of their widths up to 15 GPa and an abrupt behaviour beyond that value. Lavrentiev et al. [19] estimated that for low-energy (100 keV) C ions impinging on a Ti target the pressure increase could already reach 14 GPa, so that during irradiations with 800–900 MeV heavy ions, the outgoing pressure wave can certainly reach intensities of a few tens of GPa.

Similarly, it is interesting to compare our data with random-tiling predictions [20]. Random-tiling adepts claim that the icosahedral phase is not thermodynamically stable and that it is the rhombohedral phase that is the stable low-temperature phase. To obtain agreement with the observations they introduce the ad hoc assumption [21] that on cooling down the high-temperature icosahedral phase drops out of equilibrium. In this scenario, the dynamics become too sluggish to permit the sample to reach equilibrium, even at the slowest cooling rates that one can achieve. Our result may be contrasted with the situation in certain metastable amorphous metals where heavy-ion irradiation is able to induce crystallization [14]. If we had been able to observe a transition towards a rhombohedral phase by heavy-ion irradiation, that would have been corn on the mill of the random-tiling model. But nothing like this has been observed. As we pointed out in Section 2 it is expected to cost very little energy to create a phason defect in a QC.

Finally our data also highlight an important issue of terminology. It is customary to call (rather thoughtlessly) any peak broadening in QCs "phason broadening", which tacitly implies that it must be ascribed to phason fields. We see here that peak broadening in QCs can have also other origins. An important result of our paper is that the defects created by the irradiations are not phason defects since their intensities are not correlated with $Q_\perp$.

Acknowledgements

The authors are very grateful to the members of the CIRIL laboratory in Caen, and in particular to A. Benyayoub and J.M. Ramillon for their help during the irradiations. The kind assistance of Dominique Thiaudière during the experiments on H10 was greatly appreciated.

References

[1] R. Chatterjee, A. Kanjilal, U. Tiwari, J.M. Ramillon, A. Dunlop, Solid State Commun. 120 (2001) 289;
R. Chatterjee, A. Kanjilal, in: J. Non-Cryst. Solids, special issue for the Proceedings of the 8th International Conference on Quasicrystals (ICQ8), in press.

[2] R. Wang, X. Yang, H. Takahashi, S. Ohnuki, J. Phys.: Cond. Mat. 7 (1995) 2105;
Z. Wang, X. Yang, R. Wang, J. Phys.: Cond. Mat. 5 (1993) 7569.

[3] M. Quiquandon, A. Quivy, J. Devaud, F. Faudot, S. Lefebvre, M. Bessière, Y. Calvayrac, J. Phys.: Cond. Mat. 8 (1996) 2487;
D. Gratias, Y. Calvayrac, J. Devaud-Rzepski, F. Faudot, M. Harmelin, A. Quivy, P.A. Bancel, J. Non-Cryst. Solids 153–154 (1993) 482.

[4] A. Dunlop, D. Lesueur, P. Legrand, H. Dammak, J. Dural, Nucl. Instr. and Meth. B 90 (1994) 330;
P. Legrand, A. Dunlop, D. Lesueur, N. Lorenzelli, J. Morelli, S. Bouffard, Mater. Sci. Forum 97–99 (1992) 587.

[5] G. Coddens, S. Lyonnard, B. Hennion, Y. Calvayrac, Phys. Rev. B 62 (2000) 6268.

[6] It has been speculated many times that QCs could anneal very slowly at room temperature over long periods of time. See e.g. J. Toner, Phys. Rev. B 37 (1988) 9571.

[7] M. Boudard, M. de Boissieu, J.P. Simon, J.F. Berar, B. Doisneau, Philos. Mag. Lett. 74 (1996) 429.

[8] D.E. Cox, in: P. Coppens (Ed.), Synchrotron Radiation Crystallography, Academic Press, New York, 1992, p. 193; J.B. Hastings, W. Thomlinson, D.E. Cox, J. Appl. Cryst. 17 (1984) 85.

[9] J.W. Cahn, D. Shechtman, D. Gratias, J. Mater. Res. 1 (1986) 13.

[10] For an introduction to quasicrystallography and the importance of the $Q_\perp$ parameter we refer the reader to the reprint collection:P. Steinhardt, S. Ostlund (Eds.), The Physics of Quasicrystals, World Scientific, Singapore, 1987.

[11] T. Roisnel, J. Rodriguez-Carvajal, Mater. Sci. Forum 378–381 (2001) 118, the program is available at the web site. Available from <http://www-llb.cea.fr/fullweb/fullprof.98/fp98.htm>.

[12] M.V. Jarić, D.R. Nelson, Phys. Rev. B 37 (1988) 4458, We may note that in the derivation of this formalism one replaces generally $e^{i\mathbf{Q}\cdot\mathbf{r}}$ by $e^{i\mathbf{k}\cdot\mathbf{r}}$. This is certainly correct in

crystals where it follows from $e^{i\mathbf{G}\cdot\mathbf{r}} = 1$ and $\mathbf{k} = \mathbf{Q} - \mathbf{G}$, but not at all in QCs, which do not have translational invariance, and $|e^{i\mathbf{G}\cdot\mathbf{r}}| \neq 1$. This point has been developed by F. Ducastelle, in: Quasicrystals, Current Topics, E. Belin-Ferré, C. Berger, M. Quiquandon, A. Sadoc (Eds.), World Scientific, Singapore, 2000, p. 128. The approach of Jarić and Nelson also ignores the contribution to the signal of the atoms close to the structural defect, which undergo large displacements of the same order of magnitude as the lattice parameter. The interference between the waves scattered from such atoms and the waves scattered from the atoms that are far away from the defect (and only slightly shifted from their ideal positions) can give rise to an asymmetry in the diffuse scattering profile around the Bragg peaks, as discussed by P.H. Dederichs, J. Phys. F: Metal Phys. 3 (1973) 471. This may have a bearing on the asymmetries observed by Zhang et al. (Phys. Rev. B 66 (2002) 104202).

[13] D.S. Sivia, C.J. Carlile, W.S. Howells, S. König, Phys. B. 182 (1992) 341.

[14] M. Kopcewicz, A. Dunlop, J. Appl. Phys. 90 (2001) 74.

[15] A. Quivy, M. Quiquandon, Y. Calvayrac, F. Faudot, D. Gratias, C. Berger, R.A. Brand, V. Simonet, F. Hippert, J. Phys.: Cond. Mat. 8 (1996) 4223;
F. Puyraimond, M. Tillard, C. Bellin, M. Quiquandon, D. Gratias, A. Quivy, Y. Calvayrac, Ferroelectrics 250 (2001) 281.

[16] E.M. Bringa, in: SHIM 2002 Conference, Nucl. Instr. and Meth. B, to appear. doi:10.1016/S0168-583X(02)02006-2.

[17] R.E. Johnson, B.U.R. Sundqvist, A. Hedin, D. Fery, Phys. Rev. B 40 (1989) 49;
D. Lesueur, A. Dunlop, Radiat. Eff. Def. Solids 126 (1993) 163;
E. Bringa, R.E. Johnson, Phys. Rev. Lett. 88 (2002) 165501.

[18] For i-AlCuFe: S. Lefebvre, M. Bessière, Y. Calvayrac, J.P. Itié, A. Polian, A. Sadoc, Philos. Mag. B 72 (1995) 101;
for AlCuRu and AlPdMn: A. Sadoc, J.P. Itié, A. Polian, C. Berger, S.J. Poon, Philos. Mag. A 77 (1998) 115;
for AlCuFe approximants: J.L. Joulaud, M.J. Capitán, D. Haüsermann, Y. Calvayrac, S. Lefebvre, Phys. Rev. B 59 (1999) 3521.

[19] V. Lavrentiev, C. Hammerl, B. Rauschenbach, A. Pisanenko, O. Kukharenko, Philos. Mag. A 81 (2001) 511.

[20] M. Widom, D.P. Deng, C.L. Henley, Phys. Rev. Lett. 63 (1989) 310;
K. Strandburg, L.-H. Tang, M.V. Jarić, Phys. Rev. Lett. 63 (1989) 314.

[21] A. Letoublon, M. de Boissieu, M. Boudard, J. Gastaldi, B. Hennion, R. Caudron, R. Bellissent, Ferroelectrics 250 (2001) 261;
M. Widom, Philos. Mag. Lett. 64 (1991) 297.